



Article

Eco-Efficient Fiber-Reinforced Preplaced Recycled Aggregate Concrete under Impact Loading

Saud Alfayez ¹, Mohamed A. E. M. Ali ² and Moncef L. Nehdi ^{1,*}

¹ Department of Civil and Environmental Engineering, The University of Western Ontario, London, ON N6A 5B9, Canada; saudalfayez@gmail.com

² Department of Civil Engineering, Military Technical College, 37JW+5G Cairo, Egypt; mohamed.a.e.m.ali@gmail.com

* Correspondence: mnehdi@uwo.ca; Tel.: +519-661-2111 (ext. 88308)

Received: 25 May 2019; Accepted: 19 June 2019; Published: 21 June 2019



Abstract: This study explores highly eco-efficient preplaced aggregate concrete mixtures having superior tensile characteristics and impact resistance developed for pavement and infrastructure applications. A fully recycled granular skeleton consisting of recycled concrete aggregate and recycled tire rubber granules, and steel wire fibers from scrap tires are first placed in the formwork, then injected with a flowable grout. Considering its very high recycled content and limited mixing and placement energy (only the grout is mixed, and no mechanical vibration is needed), this material has exceptional sustainability features and offers superior time and cost savings. Moreover, typical problems of rapid loss of workability due to the high-water absorption of recycled aggregates and the floating of lightweight tire rubber granules are prevented since the aggregates are preplaced in the formwork. The much higher granular content and its denser skeleton reduce the cementitious dosage substantially and provide high volume stability against shrinkage and thermal strains. The behavior under impact loading of this sustainable preplaced recycled aggregate concrete, incorporating randomly dispersed steel wire fibers retrieved from scrap tires, was investigated using a drop weight impact test. The results show that recycled tire steel wire fibers significantly enhanced the tensile and impact properties. A two-parameter Weibull distribution provided an accurate prediction of the impact failure strength of the preplaced recycled aggregate concrete mixtures, allowing to avert additional costly laboratory experiments.

Keywords: recycled aggregate; preplaced aggregate; tire rubber; steel wire; Weibull distribution

1. Introduction

Concrete is the most widely used construction material and the world's second most consumed commodity after water. Over the last decades, reinforced concrete structures have been subjected to various extreme loading conditions, including impacts, explosions and earthquakes, which instigated several unexpected structural failures. This has escalated the impact load design requirements of concrete structures to mitigate such catastrophic failures [1–3]. Accordingly, the dynamic properties of concrete structural elements must be enhanced for better structural safety specifications [4–6].

The impact resistance of concrete is of the utmost importance for instance in transportation infrastructure and other facilities with high security standards [7]. Concrete is naturally a brittle material and can be damaged by sudden impact, which could compromise the life span of concrete elements [8]. Such a brittle characteristic of concrete generally restricts its use in dynamic applications [9]. The concept of using fibers to reinforce brittle materials has been utilized for thousands of years, for instance when sunbaked straw-fiber-reinforced bricks were used to build the 57-m high hill of Aqar-Quf in ancient Iraq [10]. Cement-based matrices have also been reinforced with asbestos and

cellulose fibers over the past century [11]. Metallic, glass, and synthetic polymer fibers have also been used to reinforce cementitious composites for several decades [10].

Many studies have demonstrated significant improvements in the impact resistance of concrete with the addition of metallic fibers [12]. Fiber-reinforced concrete exhibits extraordinary advantages pertaining to the impact resistance from the initial crack to the final failure stage [13–15]. Metallic fiber addition also enhances the fatigue, toughness and energy absorption capacity [16]. These benefits emanate primarily from the ability of fibers to arrest the initiation and propagation of cracks in cementitious matrices [12,17]. An interest in expanding research on the impact behavior of fiber-reinforced concrete escalated rapidly owing to its more ductile behavior compared to that of conventional concrete [18,19]. It is now well established that the process of concrete failure under stress depends on the fiber-matrix and aggregate-matrix bond, which control the crack pattern and mode of failure [7,20].

On the other hand, recycled rubber from scrap tires and other sources indicated promising properties for concrete under static and dynamic loading [21]. It was shown that concrete incorporating 20% of rubber, as partial replacement for sand or cement, achieved adequate engineering properties [22]. It was also observed that incorporating 50% to 75% of crumb or chipped rubber by volume of aggregate enhanced the energy absorption properties of concrete [23]. Moreover, sources of natural aggregates have been depleting in many countries, and rock extraction has led to environmental damage worldwide [24]. High demand for natural aggregate resources has contributed to raising the cost of concrete construction [25]. Hence, utilizing recycled concrete aggregates (RCA) and recycled rubber as a full or partial replacement for natural aggregates is an essential step towards sustainability and the eco-efficient management of by-products [26].

Preplaced aggregate concrete (also known as two-stage concrete, referred as TSC in the remainder of this text) has existed for several decades. Yet, its sustainability features have only been captured recently [27]. For instance, RCA and scrap tire rubber granules can be used as a full or partial replacement for natural coarse aggregates in TSC. TSC can be made by first placing the coarse aggregate in the formwork, then injecting a flowable grout to fill the voids between the aggregates, which would make the construction faster and more economical. This results in less mixing energy (only the grout is mixed), an ease of placement and no need for pumping. Workability problems associated with the loss of slump due to the high absorption of recycled aggregate, the floating of lighter rubber granules, honeycombing and segregation are all prevented since the recycled aggregate and rubber granules are preplaced in the formwork. This results in a sustainable, rapid and lower cost construction [27].

However, there is still ongoing controversy regarding the efficiency of using recycled rubber granules in concrete production, particularly with regards to the associated drop in mechanical strength [28]. Although various studies explored TSC in terms of its performance under static loading [27,29], there is a dearth of information on its performance under impact loads. Hence, in the present study, the impact resistance of sustainable TSC mixtures incorporating high recycled content (RCA, scrap tire rubber granules and steel fibers from scrap tires) have been investigated. The main objective of this study is to define sustainable concrete, not only in terms of its composition, but also its eco-efficient placement technique as a “green”, minimal cost, and possibly superior resistance to impact loading, with a focus on developing a novel, alternative construction for pavements, road barriers, and other pertinent civil infrastructures.

2. Experimental Section

2.1. Materials and Mixture Proportions

Type I portland cement (OPC) with a surface area and unit weight of $371 \text{ m}^2/\text{kg}$ and $3.15 \text{ g}/\text{cm}^3$, respectively, in accordance with the American Society for Testing and Materials ASTM C150 (Standard Specification for Portland Cement), was used in the production of TSC. The chemical composition of the cement is given in Table 1. Micro-silica sand (SS) with a maximum particle size and unit

weight of 200 μm and 2.65 g/cm^3 , respectively, was also utilized. The laser diffraction particle size distribution curves for the OPC and SS are shown in Figure 1a. A recycled concrete aggregate having a 19–38 mm particle size, unit weight of 2.60 g/cm^3 and water absorption of 2.0% was also used. Recycled granulated tire rubber was also utilized with a particle size ranging from 0.6–1.2 mm. The particle size gradation of RCA and rubber granules is shown in Figure 1b. Different TSC mixtures were prepared using the recycled granulated tire rubber with different percentages of 0%, 10%, 15%, and 20% by volume fraction. The different TSC mixtures were reinforced with recycled tire steel wire fibers having 20–45 mm in length and a mean diameter of 0.2 mm. The volume fraction of the utilized recycled tire steel wires was 0%, 0.5%, 1%, and 1.5%. A poly-carboxylate high-range water reducing admixture (HRWRA), as per the specifications of ASTM C494 (Standard Specification for Chemical Admixtures for Concrete), was added by percentage of cement weight to control the workability of the different TSC grouts. Table 2 displays the proportions of the tested TSC mixtures with a target 28-days compressive strength of 25 MPa. The first number in the mixture abbreviation relates to the recycled granulated tire rubber content, while the second shows the recycled tire steel wire content. For example, TSC20-0.5 refers to a preplaced aggregate (two-stage) concrete incorporating 20% of recycled granulated tire rubber and 0.5% recycled tire steel wires by volume fraction.

Table 1. Chemical composition of cement and silica sand.

Component (%)	Cement	Silica Sand
CaO	64.35	0.01
SiO ₂	20.08	99.70
Al ₂ O ₃	4.63	0.14
Fe ₂ O ₃	2.84	0.016
MgO	2.07	0.01
SO ₃	2.85	—
K ₂ O	—	0.04
Na ₂ O	—	0.01
Loss of ignition	2.56	—

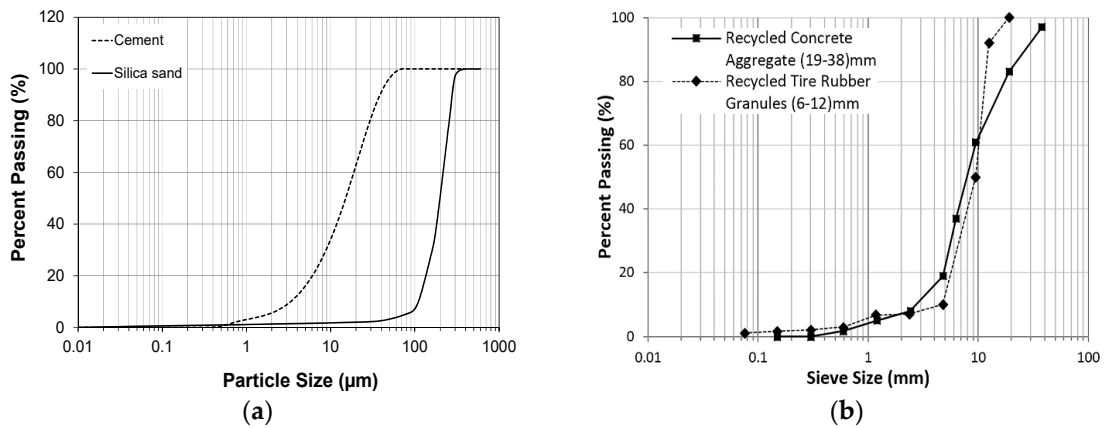


Figure 1. Particle size distribution of (a) cement and silica sand, and (b) recycled aggregate and tire rubber granules.

Table 2. Mixture proportions of the TSC mixtures.

Mixture	Cement	Silica Sand	w/cm	HRWRA	Tire Rubber (%V _f)	Steel Wires (%V _f)
TSC0-0	1.00	1.00	0.45	0.0004	0.00	0.00
TSC0-0.5	1.00	1.00	0.45	0.0004	0.00	0.50
TSC0-1	1.00	1.00	0.45	0.0004	0.00	1.00
TSC0-1.5	1.00	1.00	0.45	0.0004	0.00	1.50
TSC10-0	1.00	1.00	0.45	0.0004	10.00	0.00
TSC15-0	1.00	1.00	0.45	0.0004	15.00	0.00
TSC20-0	1.00	1.00	0.45	0.0004	20.00	0.00
TSC10-0.5	1.00	1.00	0.45	0.0004	10.00	0.50
TSC15-0.5	1.00	1.00	0.45	0.0004	15.00	0.50
TSC20-0.5	1.00	1.00	0.45	0.0004	20.00	0.50
TSC10-1	1.00	1.00	0.45	0.0004	10.00	1.00
TSC15-1	1.00	1.00	0.45	0.0004	15.00	1.00
TSC20-1	1.00	1.00	0.45	0.0004	20.00	1.00
TSC10-1.5	1.00	1.00	0.45	0.0004	10.00	1.50
TSC15-1.5	1.00	1.00	0.45	0.0004	15.00	1.50
TSC20-1.5	1.00	1.00	0.45	0.0004	20.00	1.50

2.2. Mixing and Specimen Preparation

Premixed recycled concrete aggregate, recycled tire rubber and tire steel wires were first placed in the 150 mm × 300 mm cylinders, as displayed in Figures 2 and 3. A Hobart mixer was used to dry mix the grout solid ingredients including cement and silica sand for one minute. Then, the mixing water and HRWRA were gradually added to the dry mixture over three minutes of mixing until a homogeneous mixture was achieved. Finally, the cementitious grout was injected into the forms to fill the gaps between the granules. All specimens were demolded after 24 h then placed in a 20 ± 2 °C curing room with a relative humidity of 95%, achieved using fogging nozzles, for 28 days. All reported test results represent average values obtained on identical triplicate specimens.



Figure 2. TSC specimen preparation showing preplaced aggregates in cylindrical molds (left), placement of grout by gravity (center) and final demolded specimens (right).



Figure 3. Overview of (a) tire rubber particles, and (b) preplaced RCA with scrap tire rubber granules and steel wire.

2.3. Experimental Procedures

For each TSC mixture, three 150 mm in diameter by 300 mm in height cylindrical specimens were tested at the age of 28 days to determine the compressive strength as per ASTM C39 (Standard Test Method for Compressive Strength of Cylindrical Concrete Specimens), using a standard MTS compression testing machine with a capacity of 2000 kN. Similarly, three cylindrical specimens of 150 mm × 300 mm from each TSC mixture were tested at 28 days to evaluate the elastic modulus according to ASTM C469 (Standard Test Method for Static Modulus of Elasticity and Poisson’s Ratio of Concrete in Compression). The elastic modulus for all the TSC mixtures was calculated using:

$$E = \frac{(Q_2 - Q_1)}{(\varepsilon_2 - 0.000050)} \tag{1}$$

where E is the elastic modulus in GPa, and Q_2 and Q_1 are stresses in MPa corresponding to 40% of the ultimate compressive load and a longitudinal strain of 50 millionths, respectively. ε_2 is the longitudinal strain produced by the stress Q_2 . Furthermore, three cylindrical specimens of 150 mm × 300 mm from each TSC mixture were tested at 28 days to obtain the splitting tensile strength as per ASTM C496 (Standard Test Method for Splitting Tensile Strength of Cylindrical Concrete Specimens). The splitting tensile strength was calculated as follows:

$$T = \frac{2 * P}{\pi * l * d} \tag{2}$$

where T is the splitting tensile strength in MPa, P is the maximum applied load in Newton, and l and d are the length and diameter of the cylinder in mm, respectively.

Drop weight impact testing was applied in compliance with the guidelines of the American Concrete Institute (ACI) Committee 544 (ACI Committee 544, Measurement of properties of fiber reinforced concrete) [30]. Each test specimen was adjusted in the testing setup and subjected to impact loading at 28 days, induced by a 4.5-kg impactor dropped from a height of 457 mm above the cylindrical TSC specimen, which was able to produce an impact energy of 20.167 J per hit, as shown in Figure 4. The number of impacts to induce a first visible crack (N_1), and failure (N_2), respectively was recorded. The impact energy for each TSC specimen was evaluated according to ASTM D5628 (Standard Test Method for Impact Resistance of Flat, Rigid Plastic Specimens by Means of a Falling Dart) guidelines as per the following equation:

$$IE = N_i \cdot h \cdot w \cdot f \tag{3}$$

where IE is the sustained impact energy in Joules, N_i is the number of blows, h is the falling height of the steel mass in mm, w is the mass of the steel hammer in kg, and f is a constant with a value of 9.806×10^{-3} .

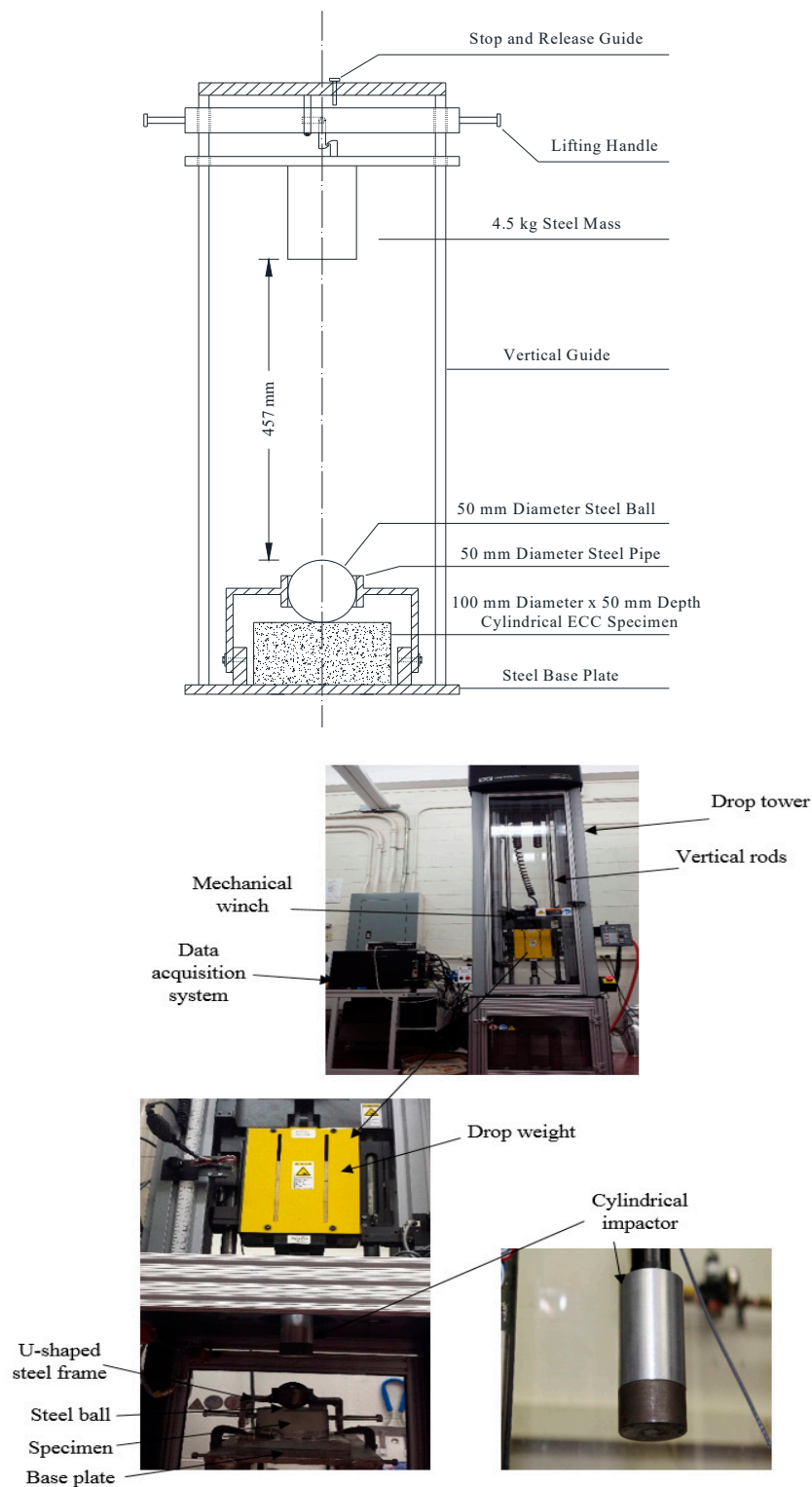


Figure 4. Schematic diagram and photographs of the drop weight impact testing system, showing the drop weight, arrangement for specimen support, and cylindrical impactor.

3. Results and Discussion

3.1. Compressive Strength

Figure 5a–c shows the variation in compressive strength for the different TSC mixtures at 28 days, which ranged from 25 to 34 MPa. Generally, steel fiber addition resulted in a slight decrease in the TSC’s compressive strength. This may be attributed to the decreased efficiency of grout filling by fibre obstruction. For instance, the compressive strength of TSC0-0.5, TSC0-1, and TSC0-1.5 decreased by 5.1%, 6%, and 6.4%, respectively, compared to that of the control TSC0-0 specimen. Similarly, the addition of recycled tire rubber decreased the compressive strength of the different TSC specimens. For example, the compressive strength of TSC10-0, TSC15-0, and TSC20-0 decreased by 10.4%, 12.5%, and 14.1% compared to that of the control TSC0-0, respectively. This can be attributed to the deformability and low stiffness of rubber granules. Incorporating a combination of recycled tire rubber and tire steel wire fibers in the TSC mixtures also decreased the compressive strength from about 35 MPa to about 28 MPa (Figure 5c).

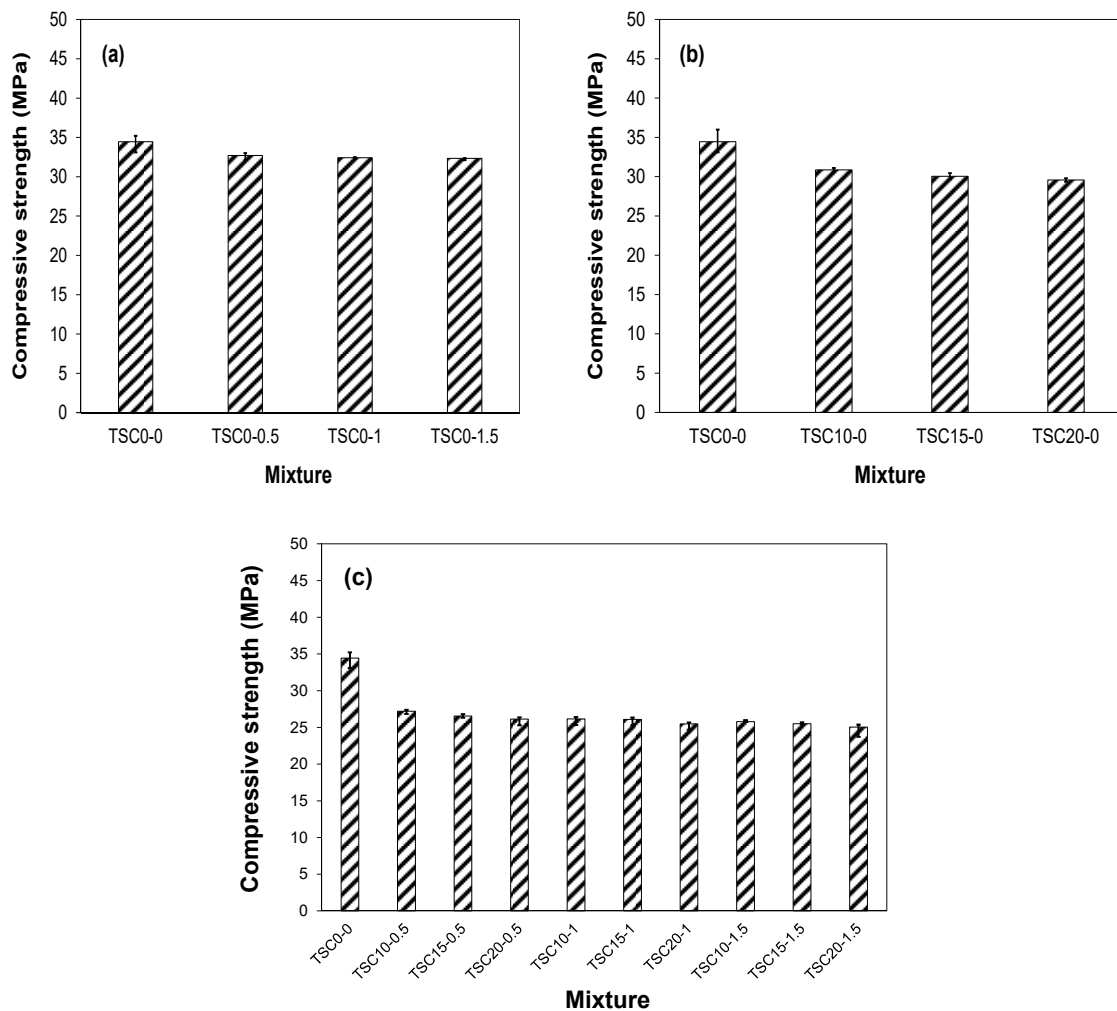


Figure 5. Compressive strength of different TSC specimens: (a) steel wires, (b) tire rubber, and (c) steel wire and tire rubber.

3.2. Elastic Modulus

The elastic modulus test results of the TSC mixtures at 28-days are displayed in Figure 6a,b. As expected, incorporating recycled tire rubber in the TSC mixtures led to a significant reduction in the elastic modulus compared to that of the rubber-less control TSC0-0 mixture. A similar trend was

observed due to a combined rubber granules and steel fiber addition (Figure 6c). For instance, the elastic modulus of TSC10-0.5, TSC15-0.5, TSC20-0.5, TSC10-1, TSC15-1, TSC20-1, TSC10-1.5, TSC15-1.5, and TSC20-1.5 specimens was lower than that of the control TSC0-0 specimens by about 21%, 23%, 24.5%, 24.2%, 24.5%, 26%, 25.1%, 26%, and 27.4%, respectively. The overall reduction in the elastic modulus of the TSC mixtures is ascribed to the low stiffness of rubber and the reduced compressive strength caused by an increased porosity associated with fiber addition.

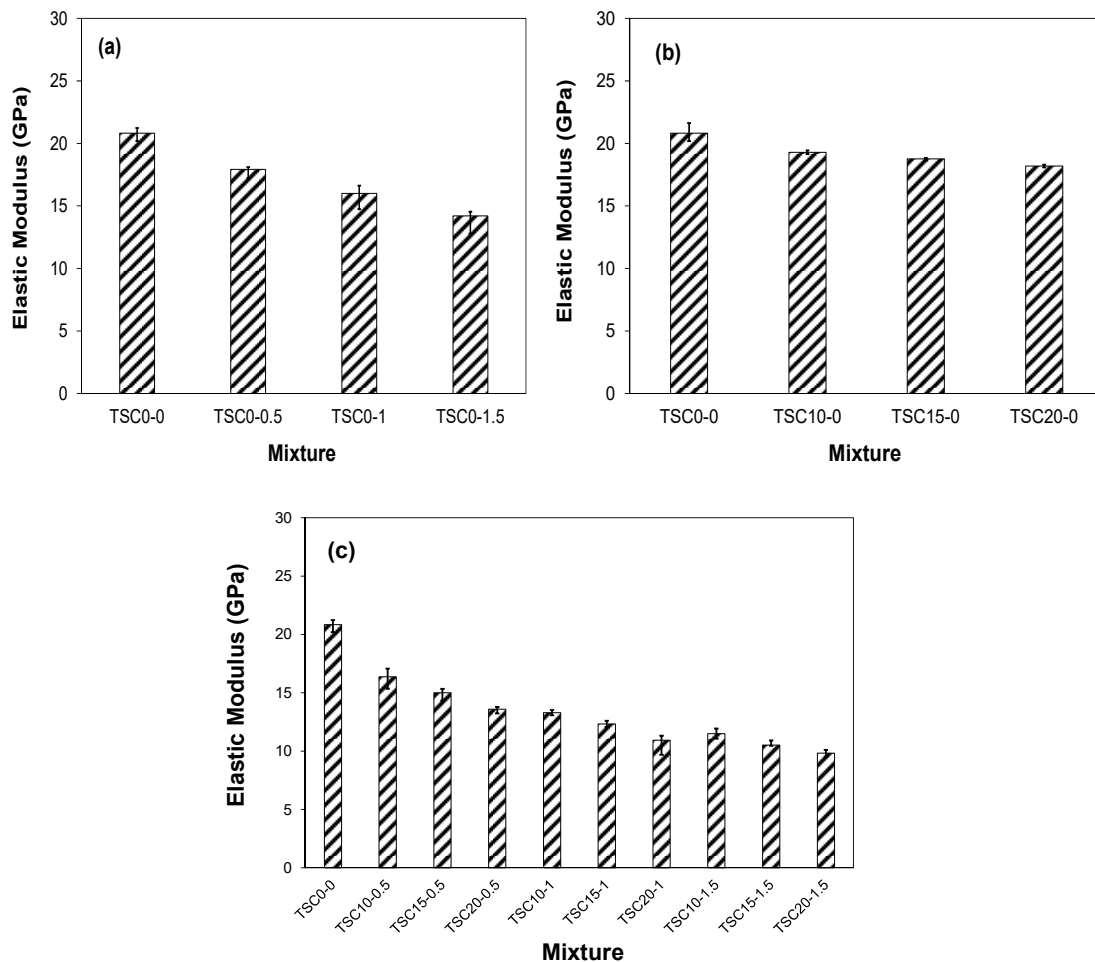


Figure 6. Elastic modulus of different TSC specimens: (a) steel wire, (b) tire rubber, and (c) combined steel wire and tire rubber.

3.3. Splitting Tensile Strength

The variation in the 28-day splitting tensile strength of the different TSC specimens is displayed in Figure 7a–c. The splitting tensile strength ranged from 3.8 to 6 MPa, as a function of the fiber dosage. It can be observed that the tensile capacity of the TSC specimens was enhanced due to the scrap tire steel wire fiber addition. For instance, the tensile capacity of the mixtures incorporating 0.5%, 1%, and 1.5% steel fibre increased by 44.7%, 50.8% and 60.5% compared to that of the control TSC0-0 mixture, respectively. This enhancement in the tensile capacity is ascribed to the fiber-matrix interfacial bond, which enhanced the load transfer across cracks with an increasing fiber content, thus improving the overall tensile load carrying capacity. Conversely, a recycled tire rubber addition induced a reduction in the splitting tensile capacity of the TSC specimens. For example, the tensile capacity of TSC10-0, TSC15-0, and TSC20-0 specimens decreased by 14%, 19.7%, and 26.3% compared to that of TSC0-0, respectively. However, the TSC specimens which incorporated a combination of recycled tire rubber and steel fiber exhibited a superior tensile capacity compared to that of the TSC control specimen.

For instance, the tensile capacity of TSC10-0.5, TSC15-0.5, TSC20-0.5, TSC10-1, TSC15-1, TSC20-1, TSC10-1.5, TSC15-1.5, and TSC20-1.5 specimens increased by about 32.5%, 19.7%, 3.7%, 36.8%, 25.8%, 5.7%, 43.9%, 33.7%, and 7.5%, compared to that of the control specimens, respectively.

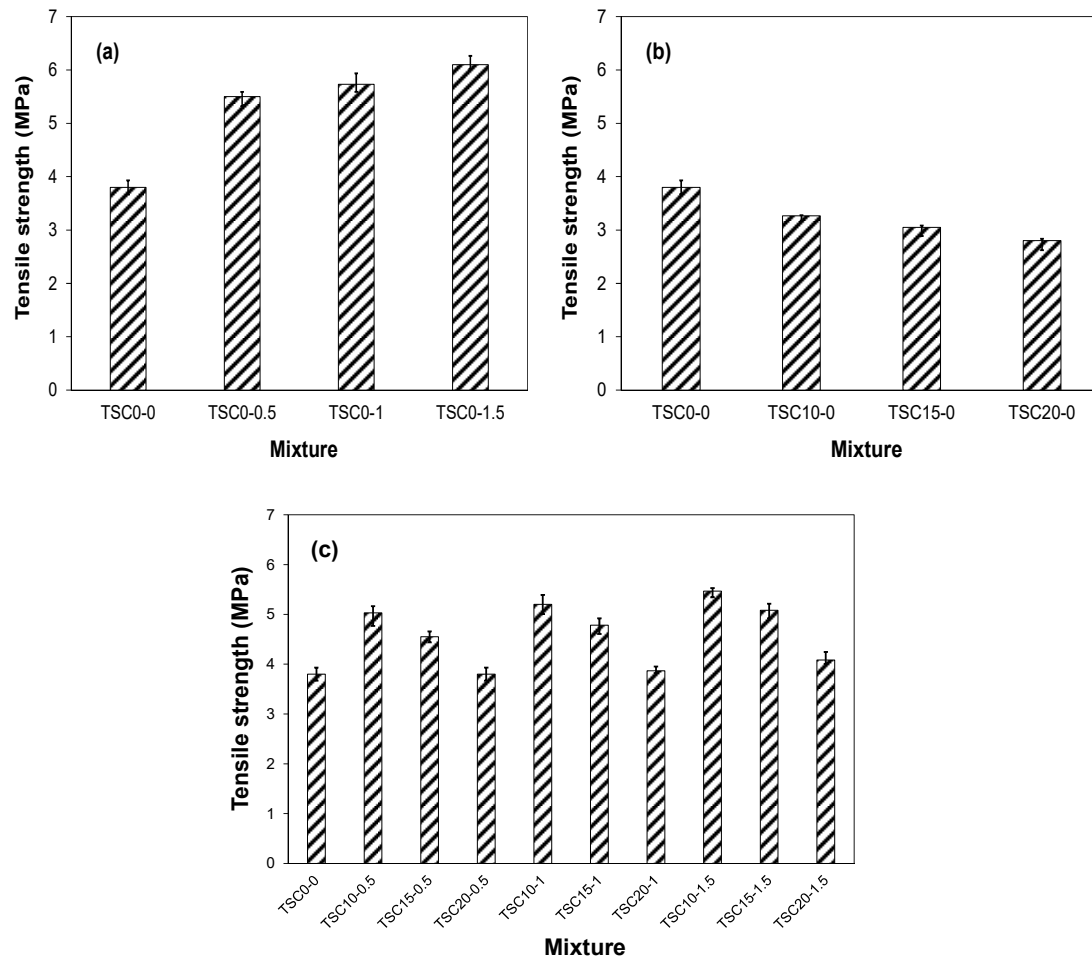


Figure 7. Tensile strength of different TSC specimens: (a) steel wires, (b) tire rubber, and (c) steel wire and tire rubber.

3.4. Impact Resistance

The behaviour of TSC specimens under impact loading was determined by evaluating their resistance to a drop weight impact as per the ACI 544 guidelines. The impact energy sustained by the different TSC specimens up to the first crack and up to failure is illustrated in Figure 8. The specimens from the fibreless control mixture (TSC0-0) failed after only one hit by the drop weight, and split into multiple fragments, which reflects its brittle nature under impact loading. Similarly, the TSC specimens which incorporated tire rubber alone followed a similar trend under impact loading, as shown in Figure 8b. Conversely, the addition of steel fiber from recycled tire wire significantly enhanced the TSC’s behaviour under impact loading by up to 40 times compared to that of the fibreless and tire rubber TSC specimens. For instance, incorporating 0.5%, 1%, and 1.5% steel fiber in TSC specimens increased their impact resistance to reach the first crack and failure by about 3, 4, and 5, and 22, 25, and 40 times that of the fibreless TSC specimens, respectively (Figure 8a). This is attributed to the ability of steel fibers to restrain crack propagation in TSC specimens under impact loading, thus altering the mode of failure from brittle to more ductile. Furthermore, incorporating a combination of recycled tire rubber and scrap tire steel wire fiber in the TSC production only led to a slight increase in the impact resistance up to the first crack compared to that of the fibreless TSC specimens (Figure 8c).

However, a significant improvement in the failure impact energy of the TSC specimens was achieved owing to combined tire rubber granules and scrap tire steel wire fiber incorporation. For instance, the energy sustained up to failure by the TSC10-0.5, TSC15-0.5, TSC20-0.5, TSC10-1, TSC15-1, TSC20-1, TSC10-1.5, TSC15-1.5, and TSC20-1.5 specimens was substantially improved by about 600%, 600%, 500%, 1000%, 700%, 700%, 1100%, 900%, and 800%, respectively (Figure 8c).

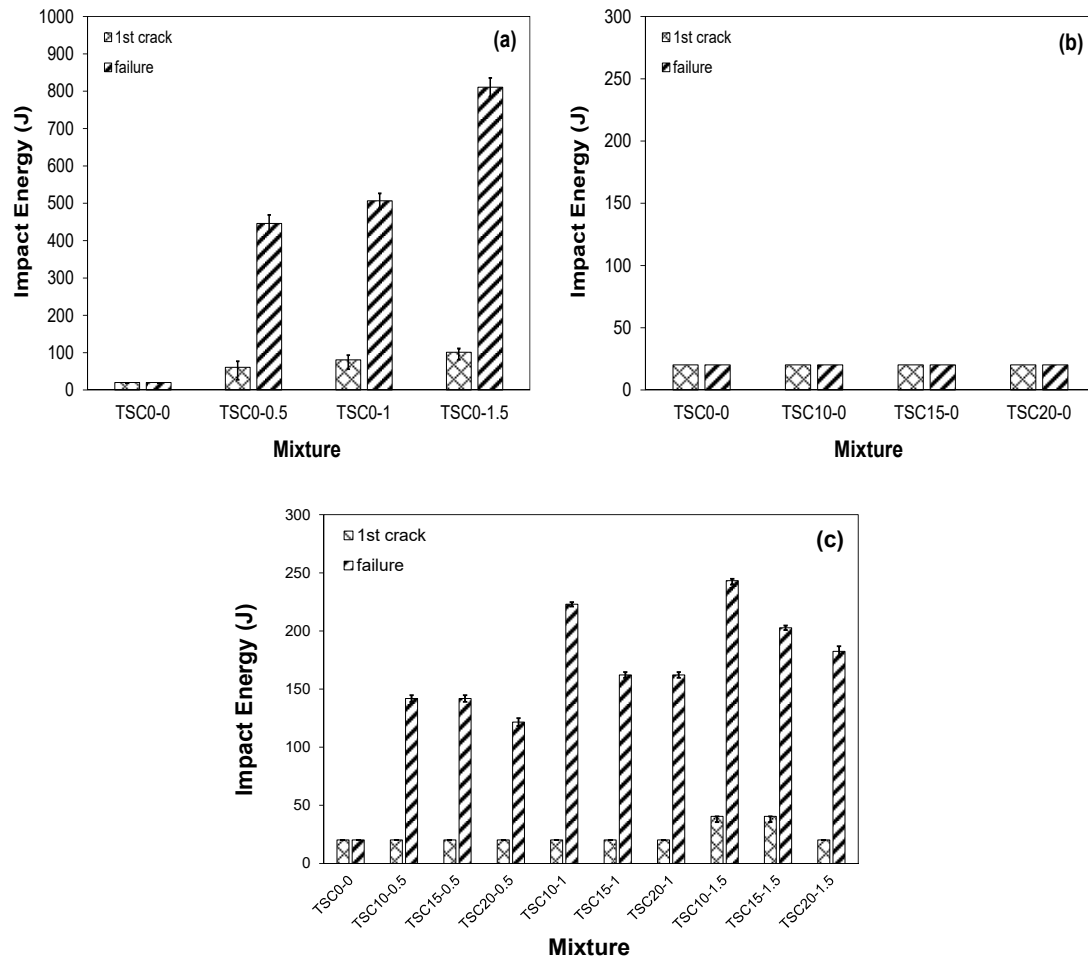


Figure 8. Impact energy sustained by different TSC specimens: (a) steel wires, (b) tire rubber, and (c) combined steel wire and tire rubber.

Generally, the tested specimens under impact loading experienced different failure patterns, as displayed in Figure 9. For instance, the fibreless TSC control specimens exhibited a brittle and sudden failure under a single impact. Incorporating tire rubber in the TSC specimens led to a similar trend. Conversely, the addition of fibers from scrap tire steel wire changed the mode of failure from a brittle mode characterised by a single crack into a ductile failure with the appearance of multiple cracking, as shown in Figure 9b–d. The number of cracks increased with an increasing steel wire volume fraction within the mixture. This can be attributed to the crack arresting capability of steel wires, which enhanced the ductile behavior and energy dissipation ability of the TSC specimens under impact loading.

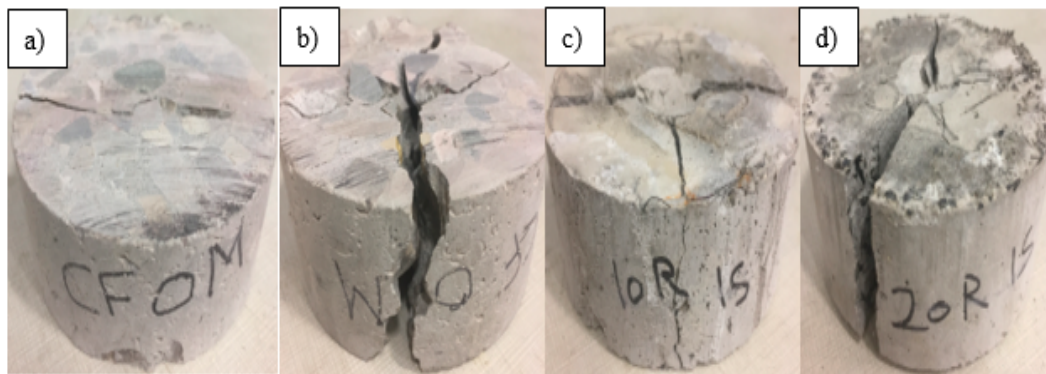


Figure 9. Failure pattern of the TSC specimens under impact loading: (a) control, (b) 0.5% steel wire, (c) 1% steel wire, and (d) 1.5% steel wire.

4. Statistical Analysis and Modeling

4.1. Analysis of Variance of Test Results

The experimental test results of concrete have been widely analyzed using different probabilistic models. Specifically, the analysis of variance (ANOVA) has been widely utilized [12,31,32]. According to ANOVA, in order to investigate whether an experimental variable, such as steel fiber addition, is statistically significant, an F_o value is estimated and compared to a standard F value of an F-distribution density function obtained from statistical tables based on the significance level (α_1) and the degrees of freedom of error determined from an experiment using the number of variables and observations. Exceeding the critical value of an F-distribution density function indicates that the tested variable significantly affects the mean of the results [33].

The F_o value can be calculated after estimating the sum of squares of the test results as follows:

$$SS_T = \left[\sum_{i=1}^a \sum_{j=1}^n y_{ij}^2 \right] - \left[\frac{y_n^2}{N} \right] \tag{4}$$

$$SS_{Treatments} = \left[\frac{1}{n} \sum_{i=1}^a y_i^2 \right] - \left[\frac{y_n^2}{N} \right] \tag{5}$$

$$SS_E = SS_T - SS_{Treatments} \tag{6}$$

where SS_T is the total corrected sum of squares, $SS_{Treatments}$ is the sum of squares due to reinforcing the specimens (e.g., different steel fiber reinforcement ratios), SS_E is the sum of squares due to error (using replicates rather than testing only one specimen), a is the number of treatments (variables), n is the number of observations (specimens), y_{ij} is the j^{th} observation taken under the factor level of the treatment i , and N is the total number of observations. The mean square of the test data can be calculated as follows:

$$MS_{Treatments} = \frac{SS_{Treatments}}{a - 1} \tag{7}$$

$$MS_E = \frac{SS_E}{N - a} \tag{8}$$

where $MS_{Treatment}$ and MS_E are the mean square due to treatments and error, respectively. The F_o value can be determined as the ratio of the mean square due to treatments to that obtained due to error as follows:

$$F_o = \frac{MS_{Treatments}}{MS_E} \tag{9}$$

ANOVA at a significance level $\alpha_1 = 0.05$ indicated that the variation in the dosage of recycled steel wire fiber had an insignificant effect on the mean value of the compressive strength of the TSC

concrete. The obtained F_o value for the compressive strength results was 3.96, which is lower than the corresponding critical F value of 4.46 ($F_{0.05,2,8}$). Conversely, the variation in the addition level of steel wire fiber showed a significant effect on the splitting tensile strength and impact resistance of the TSC concrete. The determined F_o values for the splitting tensile strength and impact resistance were 31.87 and 117.6, respectively. On the other hand, incorporating tire rubber granules in TSC specimens indicated an insignificant effect on the mean value of the compressive and splitting tensile strengths and on the impact resistance of the TSC specimens, with corresponding F_o values of 1.52, 2.1 and 2, respectively, which is lower than the corresponding critical $F_{0.05,2,8}$ value.

4.2. Weibull Distribution Model

Different probabilistic models have been utilized to statistically analyze the impact test data of concrete materials, among which the two-parameter Weibull distribution was widely utilized by several researchers for estimating the impact performance of concrete (e.g., [34–36]). The Weibull distribution function is determined by a probability density function $f(n)$ as follows:

$$f(n) = \frac{\alpha}{u} \left(\frac{n}{u}\right)^{\alpha-1} e^{-\left(\frac{n}{u}\right)^\alpha} \tag{10}$$

where α is the shape parameter (i.e., Weibull slope), u describes the scale parameter, and n is the specific value of the random variable N (i.e., N_1 and N_2 in this study). By integrating Equation (10), Equation (11) can be determined:

$$F_N(n) = 1 - e^{-\left(\frac{n}{u}\right)^\alpha} \tag{11}$$

where $F_N(n)$ describes the cumulative distribution function. The probability of survivorship function is estimated using Equation (12), according to Saghafi et al. [37]:

$$L_N = 1 - F_N(n) = e^{-\left(\frac{n}{u}\right)^\alpha} \tag{12}$$

Equation (12) can be rewritten by taking the natural logarithm twice on both sides as follows:

$$\ln \left[\ln \left(\frac{1}{L_N} \right) \right] = \alpha \ln(n) - \alpha \ln(u) \tag{13}$$

In order to estimate Equation (13) graphically, the empirical survivorship function L_N for the impact test data is determined from the following relation [36]:

$$L_N = 1 - \frac{i - 0.3}{k + 0.4} \tag{14}$$

where i is the failure order number, and k represents the number of data points. According to Figures 10 and 11, a linear regression analysis was applied to the $\ln [\ln (1/L_N)]$ and $\ln (\text{impact energy})$ values. The linear trend is established by drawing the best fit line between the data points using the method of least squares. The slope of the line provides an estimate of the shape parameter (α) and the scale parameter (u), which can be determined by calculating the value at which the line intersects the $\ln [\ln (1/L_N)]$ axis. The shape parameter (α), scale parameter (u) and the coefficient of determination (R^2) for the TSC specimens are presented in Table 3.

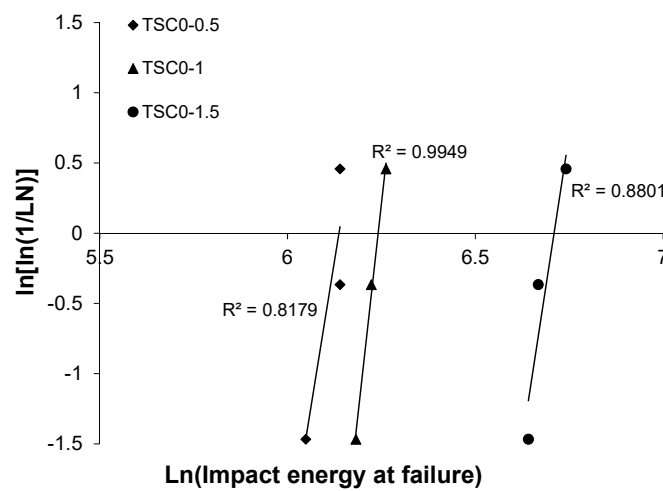


Figure 10. Weibull distribution of steel wires for the TSC specimens.

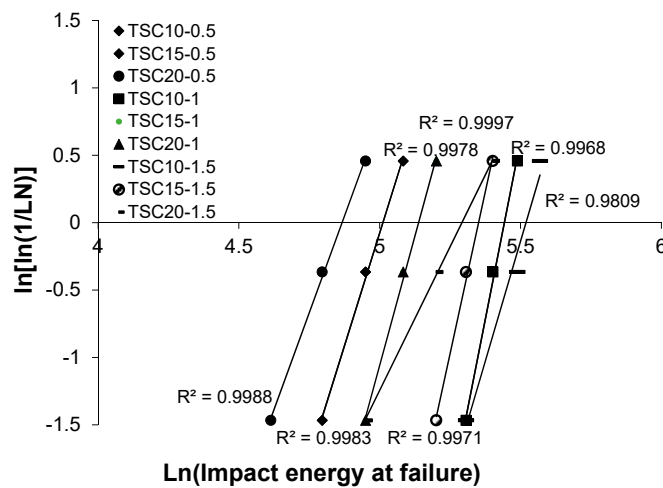


Figure 11. Weibull distribution of steel wires and tire rubber for the TSC specimens.

Table 3. Shape, scale parameters and coefficient of determination of the TSC specimens.

Specimen ID	α	u	R^2
TSC0-0.5	16.632	-102.06	0.8179
TSC0-1	24.071	-150.2	0.9949
TSC0-1.5	17.447	-117.1	0.8801
TSC10-0.5	6.7033	-33.594	0.9983
TSC15-0.5	6.7033	-33.594	0.9983
TSC20-0.5	5.731	-27.89	0.9988
TSC10-1	10.575	-57.553	0.9968
TSC15-1	7.6731	-39.425	0.9978
TSC20-1	7.6731	-39.425	0.9978
TSC10-1.5	7.1142	-39.266	0.9809
TSC15-1.5	9.6084	-51.415	0.9971
TSC20-1.5	4.6243	-22.566	0.9997

The estimated impact energy values for the TSC specimens at the failure stage are displayed in Tables 4 and 5 based on the reliability analysis. The first crack impact energy of TSC0-0.5, TSC0-1, and TSC0-1.5 specimens was approximately equal to or higher than 68.633, 89.147, and 109.544 J with an R^2 of 0.9998, 0.9999, and 0.9994, respectively. Furthermore, the impact energy at failure of TSC0-0.5, TSC0-1, and TSC0-1.5 specimens was approximately equal to or higher than 462.36, 513.64,

and 820.585 J with an R^2 of 0.8179, 0.9949, and 0.8801, respectively. As indicated by others (e.g., [38,39]), a coefficient of determination R^2 of 0.7 or higher is sufficient for a reasonable reliability model. Since all impact test data had an R^2 equal to or higher than 0.8179, a two-parameter Weibull distribution could be used to estimate the statistical distribution of the impact test results for TSC concrete. In addition, the developed reliability curves may provide a useful tool to determine the impact resistance of TSC at first cracking and failure, without the need for costly and time-consuming additional impact testing.

Table 4. Weibull distribution for impact energy of recycled tire steel wire reinforced TSC specimens.

Reliability Level	TSC0-0.5	TSC0-1	TSC0-1.5
0.99	350.647	424.295	630.411
0.90	403.857	467.803	721.298
0.80	422.496	482.616	753.000
0.70	434.579	492.112	773.516
0.60	444.067	499.511	789.607
0.50	452.292	505.885	803.542
0.40	459.945	511.784	816.499
0.30	467.558	517.623	829.378
0.20	475.790	523.902	843.291
0.10	486.146	531.756	860.781
0.01	506.835	547.291	895.667

Table 5. Weibull distribution for impact energy (J) of various TSC specimens.

Reliability Level	TSC0-0.5	TSC10-0.5	TSC20-0.5	TSC0-0.5	TSC10-0.5	TSC20-0.5	TSC0-0.5	TSC10-0.5	TSC20-0.5
0.99	75.5889	75.5889	58.1972	149.5097	93.5563	93.5563	130.682	130.619	48.6716
0.90	107.324	107.324	87.6937	186.7112	127.078	127.078	181.828	166.807	80.9016
0.80	120.037	120.037	99.9621	200.4421	140.134	140.134	202.056	180.357	95.1556
0.70	128.736	128.736	108.487	209.5320	148.967	148.967	215.826	189.379	105.313
0.60	135.823	135.823	115.504	216.7714	156.106	156.106	227.003	196.593	113.819
0.50	142.15	142.15	121.822	223.1190	162.441	162.441	236.954	202.938	121.585
0.40	148.194	148.194	127.902	229.0859	168.458	168.458	246.434	208.919	129.149
0.30	154.355	154.355	134.143	235.0780	174.561	174.561	256.076	214.942	137.005
0.20	161.185	161.185	141.112	241.6197	181.29	181.29	266.74	221.534	145.88
0.10	170.031	170.031	150.212	249.9428	189.953	189.953	280.513	229.947	157.627
0.01	188.554	188.554	169.524	266.8744	207.911	207.911	309.219	247.148	183.117

5. Conclusions

This study investigated the behaviour of sustainable preplaced recycled aggregate concrete (TSC) reinforced with recycled tire steel wire fibers under static and impact loading. The TSC concrete was exclusively made with RCA and 0%, 10%, 15%, and 20% of recycled tire rubber granules, along with 0%, 0.5%, 1% and 1.5% (by volume fraction) of recycled steel wire fibers from scrap tires. In addition to its very high recycled content and exceptional sustainability features, this material can offer unique time and cost savings for pavement and sidewalk construction. Only a grout needs mixing, while the aggregates can be preplaced like road bases. Typical problems related to the high-water absorption of recycled aggregates and the floating of tire rubber granules in normal concrete mixtures are avoided since the aggregates are preplaced. The dense granular structure reduces the cementitious content substantially and could provide volume stability against shrinkage and thermal strains. Based on the experimental findings, the conclusions below can be drawn:

- The compressive strength of TSC specimens decreased due to the tire rubber addition, while the steel wire fiber addition did not have a significant effect on the compressive strength.
- The tensile strength of the sustainable TSC specimens was significantly enhanced by up to 58% owing to the recycled steel wire fiber addition. ANOVA confirmed that incorporating recycled steel wire fiber in the TSC mixtures had a significant positive effect on the tensile capacity of the

TSC. Among all of the tested specimens, TSC incorporating no tire rubber and 1.5% steel fiber achieved the highest tensile capacity.

- The behavior of TSC subjected to impact loading was enhanced by 22 to 40 times owing to the steel fiber addition. However, incorporating tire rubber in TSC decreased its impact performance.
- The Weibull distribution function achieved an adequate capability of representing the impact test data of TSC with a linear correlation between the numbers of impacts that initiated ultimate failure for all TSC specimens.
- The study pioneers a highly sustainable concrete with entirely recycled granular content, entirely recycled fibre reinforcement, and a large volume recycled binder, with a sustainable low energy mixing requirement and placement, superior tensile properties and impact resistance for the protection of civil infrastructures in the event of unexpected severe loading conditions, while valorizing waste and by-products and lowering the energy used in concrete production and placement, as well as the overall material intensity.
- A potential application of this highly eco-efficient concrete would be for pavements and sidewalks, road barriers, and protective systems for critical infrastructures against impacts.

Author Contributions: S.A. conducted the experimental work, formal analysis of results and writing the initial draft of the manuscript. M.A.E.M.A. Aly conducted the impact testing investigation, and the formal analysis, discussion and writing of the impact test sections. M.L.N. was responsible for conceptualization, methodology, validation, review and editing, supervision, project administration, and writing of the final version of the manuscript.

Funding: There was no external funding for this study.

Conflicts of Interest: The authors have no conflict of interest to declare.

References

1. Adhikary, S.D.; Li, B.; Fujikake, K. State-of-the-art review on low-velocity impact response of reinforced concrete beams. *Mag. Concr. Res.* **2016**, *68*, 701–723. [[CrossRef](#)]
2. Alhadid, M.M.A.; Soliman, A.M.; Nehdi, M.L.; Youssef, M.A. Critical overview of blast resistance of different concrete types. *Mag. Concr. Res.* **2014**, *66*, 72–81. [[CrossRef](#)]
3. Remennikov, A.; Kaewunruen, S. Impact resistance of reinforced concrete columns: Experimental studies and design considerations. In Proceedings of the 19th Australasian Conference on the Mechanics of Structures and Materials, Christchurch, New Zealand, 29 November–1 December 2006; pp. 817–824.
4. Kennedy, R.P. A review of procedures for the analysis and design of concrete structures to resist missile impact effects. *Nucl. Eng. Des.* **1976**, *37*, 183–203. [[CrossRef](#)]
5. Li, Q.M.; Reid, S.R.; Wen, H.M.; Telford, A.R. Local impact effects of hard missiles on concrete targets. *Int. J. Impact Eng.* **2005**, *32*, 224–284. [[CrossRef](#)]
6. Luccioni, B.M.; Ambrosinia, R.D.; Danesia, R.F. Analysis of building collapse under blast loads. *Eng. Struct.* **2004**, *26*, 63–71. [[CrossRef](#)]
7. Murali, G.; Santhi, A.S.; Ganesh, G.M. Impact resistance and strength reliability of fiber-reinforced concrete in bending under drop weight impact load. *Int. J. Technol.* **2014**, *5*, 111–120. [[CrossRef](#)]
8. Murnal, P.B.; Chatorikar, R.N. Impact resistance of steel fiber reinforced concrete. *Int. J. Res. Eng. Technol.* **2015**, *4*, 241–246.
9. Chen, Y.; May, I.M. Reinforced concrete members under drop-weight impacts. *Struct. Build.* **2009**, *162*, 45–56. [[CrossRef](#)]
10. Hannant, D.J. Fibre reinforcement in the cement and concrete industry. *Mater. Sci. Technol.* **1995**, *11*, 853–861. [[CrossRef](#)]
11. MacVicar, R.; Matuana, L.M.; Balatinecz, J.J. Aging mechanism in cellulose fiber reinforcement cement composite. *Cem. Concr. Compos.* **1999**, *21*, 189–196. [[CrossRef](#)]
12. Ali, M.A.E.M.; Nehdi, M.L.; Soliman, A.M. Exploring behavior of novel hybrid-fiber reinforced engineered cementitious composite under impact loading. *Mater. Des.* **2017**, *117*, 139–149. [[CrossRef](#)]

13. Mahmoud, N.; Afroughsabet, V. Combined effect of silica fume and steel fibers on the impact resistance and mechanical properties of concrete. *Int. J. Impact Eng.* **2010**, *37*, 879–886.
14. Taner, Y.S.; Cevdet, E.E.; Findik, F. Properties of hybrid fiber reinforced concrete under repeated impact loads. *Russ. J. Nondestruct. Test.* **2010**, *46*, 538–546. [[CrossRef](#)]
15. Alavi, N.A.; Hedayatian, M.; Mahmoud, N.; Afrough, S.V. An experimental and numerical study on how steel and polypropylene fibers affect the impact resistance in fiber-reinforced concrete. *Int. J. Impact Eng.* **2012**, *46*, 62–73. [[CrossRef](#)]
16. Ali, M.A.E.M.; Nehdi, M.L. Innovative self-healing hybrid fiber reinforced engineered cementitious composite. *Constr. Build. Mater.* **2017**, *150*, 689–702. [[CrossRef](#)]
17. Rao, B.K.; Ravindra, V.; Rajagopal, A. Experimental investigation on impact strength of steel fiber reinforced normal and self-compacting concrete. *Int. J. Civ. Eng. Archit.* **2012**, *2*, 495–505.
18. Adhikary, S.D.; Li, B.; Fujikake, K. Residual resistance of impact-damaged reinforced concrete beams. *Mag. Concr. Res.* **2015**, *67*, 364–378. [[CrossRef](#)]
19. Swamy, R.N.; Jojagha, A.H. Impact resistance of steel fibre reinforced lightweight concrete. *Int. J. Cem. Compos. Lightweight Concr.* **1982**, *4*, 209–220. [[CrossRef](#)]
20. Yew, M.K.; Othman, I.; Yew, M.C.; Yeo, S.H.; Mahmud, H. Strength properties of hybrid nylon-steel and polypropylene-steel fibre-reinforced high strength concrete at low volume fraction. *Int. J. Phys. Sci.* **2011**, *6*, 7584–7588.
21. Khalil, E.; Abd-Elmohsen, M.; Anwar, A.M. Impact resistance of rubberized Self-compacting concrete. *Water Sci.* **2015**, *29*, 45–53. [[CrossRef](#)]
22. Al-Tayeb, M.M.; Abu-Bakar, B.H.; Ismail, H.; Akil, H.M. Impact resistance of concrete with partial replacements of sand and cement by waste rubber. *Polym. Plast. Technol. Eng.* **2012**, *51*, 1230–1236. [[CrossRef](#)]
23. Reda-Taha, M.M.; El-Dieb, A.S.; Abdel-Wahab, M.A.; Abdel-Hameed, M.E. Mechanical, fracture, and microstructural investigations of rubber concrete. *J. Mater. Civ. Eng.* **2008**, *20*, 640–649. [[CrossRef](#)]
24. Vadivel, T.S.; Thenmozhi, R.; Doddurani, M. Experimental behavior of waste tire rubber aggregate concrete under impact loading. *IJST Trans. Civ. Eng.* **2014**, *38*, 251–259.
25. Abdullah, S.R.; Zainal-Abidin, W.R.W.; Shahidan, S. Strength of concrete containing rubber particle as partial cement replacement. In Proceedings of the 3rd International Conference on Civil and Environmental Engineering for Sustainability, Melaka, Malaysia, 1–2 December 2015; Volume 47, pp. 1–4.
26. Yehia, S.; Helal, K.; Abusharkh, A.; Zaher, A.; Istaitiyeh, H. Strength and durability evaluation of recycled aggregate concrete. *Int. J. Concr. Struct. Mater.* **2015**, *9*, 219–239. [[CrossRef](#)]
27. Nehdi, M.L.; Najjar, M.F.; Soliman, A.M.; Azabi, T.M. Novel steel fibre-reinforced preplaced aggregate concrete with superior mechanical performance. *Cem. Concr. Compos.* **2017**, *82*, 242–251. [[CrossRef](#)]
28. Ismail, S.; Ramli, M. Impact resistance of recycled aggregate concrete with single and hybrid fibers. In Proceedings of the 3rd International Conference on Civil and Environmental Engineering for Sustainability, Melaka, Malaysia, 1–2 December 2015; Volume 47, pp. 1–7.
29. Liu, F.; Chen, G.; Li, L.; Guo, Y. Study of impact performance of rubber reinforced concrete. *Constr. Build. Mater.* **2012**, *36*, 604–616. [[CrossRef](#)]
30. ACI Committee 544. *Measurement of Properties of Fiber Reinforced Concrete*; 48331-3439, ACI Standard 544.2R-89 (Reapproved 2009); American Concrete Institute: Farmington Hills, MI, USA, 1999.
31. Ahmad, S.; Alghamdi, S.A. A statistical approach to optimizing concrete mixture design. *Sci. World J.* **2014**, *2014*, 561539. [[CrossRef](#)]
32. Soliman, A.M.; Nehdi, M.L. Effect of natural wollastonite microfibers on early age behavior of UHPC. *J. Mater. Civ. Eng.* **2012**, *24*, 816–824. [[CrossRef](#)]
33. Montgomery, D.C. *Design and Analysis of Experiments*, 8th ed.; John Wiley and Sons: Hoboken, NJ, USA, 2012.
34. Li, H.; Zhang, M.; Ou, J. Flexural fatigue performance of concrete containing nanoparticles for pavement. *Int. J. Fatigue* **2007**, *29*, 1292–1301. [[CrossRef](#)]
35. Raif, S.; Irfan, A. Statistical analysis of bending fatigue life data using Weibull distribution in glass-fiber reinforced polyester composites. *Mater. Des.* **2008**, *29*, 1170–1181.
36. Raman, B.; Rakesh, C. Fatigue-life distributions and failure probability for glass-fiber reinforced polymeric composites. *Compos. Sci. Technol.* **2009**, *69*, 1381–1387.
37. Saghafi, A.; Mirhabibi, A.R.; Yari, G.H. Improved linear regression method for estimating Weibull parameters. *Theor. Appl. Fract. Mech.* **2009**, *52*, 180–182. [[CrossRef](#)]

38. Rahmani, T.; Kiani, B.; Shekarchi, M.; Safari, A. Statistical and experimental analysis on the behavior of fiber reinforced concretes subjected to drop weight test. *Constr. Build. Mater.* **2012**, *37*, 360–369. [[CrossRef](#)]
39. Chen, X.; Ding, Y.; Azevedo, C. Combined effect of steel fibres and steel rebars on impact resistance of high-performance concrete. *J. Cent. South Univ. Technol.* **2011**, *18*, 1677–1684. [[CrossRef](#)]



© 2019 by the authors. Licensee MDPI, Basel, Switzerland. This article is an open access article distributed under the terms and conditions of the Creative Commons Attribution (CC BY) license (<http://creativecommons.org/licenses/by/4.0/>).